International Journal of Fluid Power 1 (2000) No. 1 pp. 27-38

INVESTIGATIONS OF THE TEMPERATURE BEHAVIOUR OF THE PISTON CYLINDER ASSEMBLY IN AXIAL PISTON PUMPS

Lars Olems

Technical University of Hamburg-Harburg, Institute for Aircraft Systems Engineering, Neßpriel 5, 21129 Hamburg, Germany
L.Olems@tu-harburg.de

Abstract

In this paper the temperature behaviour of the piston cylinder assembly in swash plate type axial piston pumps is investigated. For the theoretical investigations a mathematical model is used that allows the calculation of the nonisothermal gap flow between piston and cylinder. For this purpose the Reynolds Equation, the energy equation and the equations of motion have to be solved. The gap flow and the pressure distribution in the gap is calculated by solving the Reynolds Equation numerically with a finite volume method. The temperature distribution is obtained by solving the energy equation over the piston cylinder assembly also numerically with a finite volume method. It is known that the piston undergoes an eccentric motion in the cylinder that has a significant influence on the gap flow. To calculate this motion a simplified equation of motion, based on the external forces, the hydrodynamic forces and the forces caused by elastic deformation, is used. A method is described that combines the calculation of these three equations and that allows calculation of the gap flow and the temperature distribution in the assembly depending on the design and the operating parameters of the machine. The experimental investigations were made on a standard pump that was modified for the measurements. The temperature distributions in the whole cylinder block of the machine and the dynamic pressure in the displacement chamber were measured under real operating conditions using a telemetry unit. The results were used to verify the simulation model.

Keywords: axial piston machine, piston cylinder assembly, nonisothermal gap flow, Reynolds Equation, energy equation, temperature distribution.

1 Introduction

One aim in designing axial piston pumps is to improve efficiency and reliability, and to increase the working pressure and the swash plate angle of the machines (Ivantysynova 1999a). The gap between pump piston and cylinder is one important part in the machine (see Fig. 1). It has an influence on the operating parameters and the efficiency. It is important for carrying the high radial loads that are typical for swash plate type machines and for sealing the high pressure in the displacement chamber. Due to the piston motion a hydrodynamic flow field is established in the gap that carries radial loads. Because the loads are changing while the shaft of the machine rotates, the piston executes very small radial motions in the cylinder. This motion has an essential influence on the shape of the gap and the pressure distribution in the gap.

Although models for calculating the gap flow are existing, the design of the gap size is based on experimental investigations. Renius (1974) e.g. made extensive experimental and theoretical investigations on the friction behaviour of the piston cylinder assembly using a one-piston model pump. Ivantysynova (1985) used a model based on the simultaneous solution of the Reynolds Equation and the energy equation for calculating the nonisothermal gap flow. She made experimental investigations to measure the temperature and pressure distribution in the gap. The results were used to verify her calculations. Kleist (1995) has specified an isothermal method for calculating the eccentric motion of the pump piston in the gap with two degrees of freedom in a radial piston machine. He compared his results to experimental investigations that were made on a especially designed model pump.

In this paper a nonisothermal method for the calculation of the gap flow and the pressure distribution in the gap between piston and cylinder in swash plate type axial piston machines is presented. The temperature distribution in the gap flow, in the piston and in the cylinder block is calculated. The calculation method is based on known values of the assembly geometry, the

This manuscript was received on 16 October1999 and was accepted after revision for publication on 18 January 2000

machine operating parameters and the case temperature. The developed model considers the eccentric motion of the piston in the cylinder with four degrees of freedom. It is calculated by solving the equations of the eccentric motion of the piston. It is shown that the equations of motion can be simplified by neglecting the inertial forces which result from this motion. The strong dependency of the oil viscosity from the local temperature is taken into account by using a thermal model that computes the temperature in the whole assembly. It considers the heat dissipated in the gap flow, the material properties, the heat conduction and the heat transmission on the surface of the cylinder block. The thermal model is confirmed with measurements made by the author on a modified pump. The pump is operated under normal operating conditions. A special test rig using a telemetry unit for transferring the signals from the rotating cylinder block was realised in the laboratory of the Institute of Aircraft Systems Engineering at the Technical University of Hamburg-Harburg.

2 Operation of the Machine and Loads

Figure 1 shows the piston cylinder assembly of a swash plate type axial piston pump. When the machine is operated, the cylinder block slides over the valve plate. The displacement chambers of each piston are connected to the high-pressure port or the low-pressure port. The pistons are joined to the slippers that glide over the swash plate. By changing the swash plate angle ß, the piston stroke can be adjusted. In the pump investigated in this study the pistons are tilted with an angle ε to the shaft to improve the suction behaviour. For the description of the kinematics, a co-ordinate system is established that rotates with the cylinder block and has its origin on the axis of the cylinder bore. One can derive analytical expressions for the piston displacement s_K, the piston velocity v_K and the piston

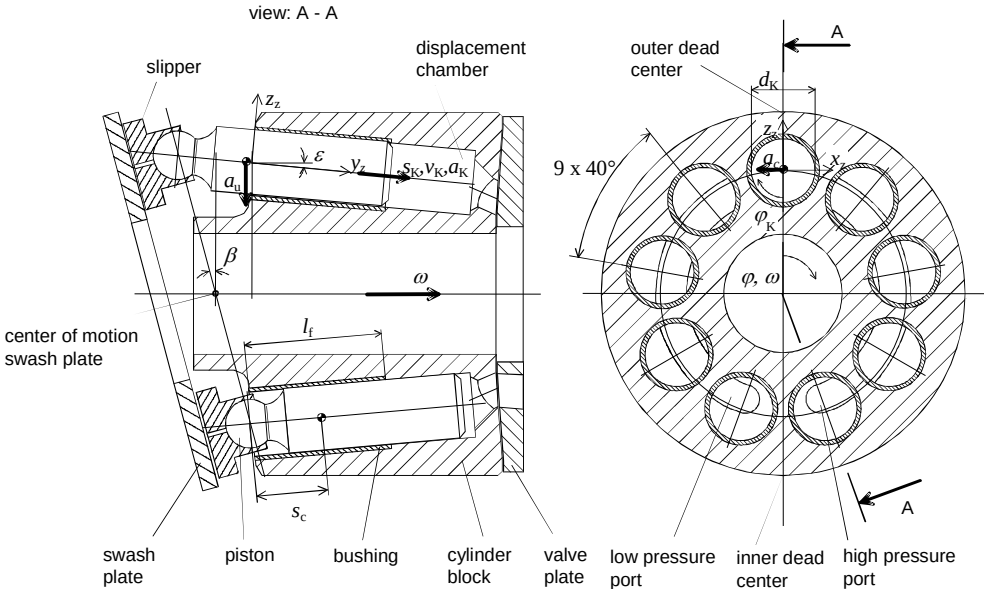

Fig. 1: *Piston cylinder assembly*

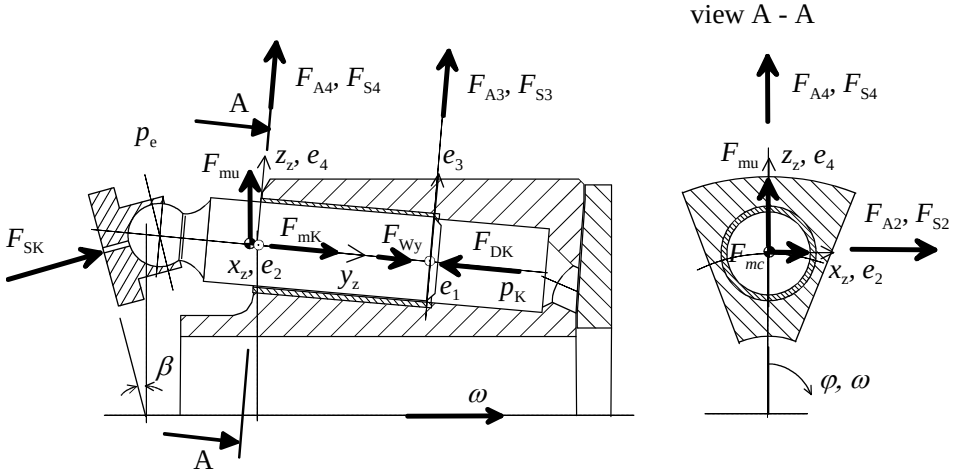

Fig. 2: *Piston forces*

accelerations a_K, a_u and a_c (see Ivantysyn and Ivantysynova 1993). Here the Coriolis acceleration a_c occurs, because the piston velocity v_K has a component normal to the vector of the rotational speed ω of the cylinder block. The rotational speed of the piston is not determined by the kinematics of the assembly. It is determined by the sum of all friction forces acting on the piston (Renius, 1974). Here it is assumed that the piston rotates relatively to the cylinder block with the rotational speed of the machine.

Figure 2 shows the forces that are acting on the piston cylinder assembly. The main external forces are the pressure force F_{DK} and the inertial forces F_{mu}, F_{mc} and F_{mK}. Removing the swash plate one can calculate the reaction force F_{SK} that is acting on the slipper. The pressure force F_{DK} is calculated with the pressure difference between the casing and the displacement chamber.

$$F_{DK} = \frac{\pi}{4} \cdot d_K^2 \cdot \left(p_K - p_e\right) \tag{1}$$

The inertial forces can be directly calculated with the piston accelerations a_u, a_c and a_K:

$$F_{mK} = -a_K \cdot m_K \tag{2}$$

$$F_{mu} = a_u \cdot m_K \tag{3}$$

$$F_{mc} = a_c \cdot m_K \tag{4}$$

The sum of forces acting in the axial piston direction is:

$$F_{Ry} = -F_{DK} + F_{mK} + F_{Wy} - F_{mu} \cdot \sin\varepsilon \tag{5}$$

For the calculation of the motion of the piston it is necessary to know the forces that are acting on the piston cylinder assembly. The pressure force and the inertial forces can be resolved into the forces F_{A1} to F_{A4}:

$$F_{A1} = -F_{Ry} \cdot \frac{\tan\beta \cdot \cos\varphi}{\cos\varepsilon \cdot \left(1 - \tan\varepsilon \cdot \tan\beta \cdot \cos\varphi\right)} \cdot \frac{s_K}{l_f} - F_{mc} \cdot \frac{s_K + s_c}{l_f} \tag{6}$$

$$F_{A2} = -F_{Ry} \cdot \frac{\tan\beta \cdot \cos\varphi}{\cos\varepsilon \cdot \left(1 - \tan\varepsilon \cdot \tan\beta \cdot \cos\varphi\right)} \cdot \left(1 - \frac{s_K}{l_f}\right) - F_{mc} \cdot \left(1 - \frac{s_K + s_c}{l_f}\right) \tag{1}$$

$$F_{A3} = F_{Ry} \cdot \frac{\tan\beta \cdot \cos\varphi + \tan\varepsilon}{1 - \tan\varepsilon \cdot \tan\beta \cdot \cos\varphi} \cdot \frac{s_K}{l_f} - F_{mu} \cdot \cos\varepsilon \cdot \frac{s_K + s_c}{l_f} \tag{2}$$

$$F_{A4} = F_{Ry} \cdot \frac{\tan\beta \cdot \cos\varphi + \tan\varepsilon}{1 - \tan\varepsilon \cdot \tan\beta \cdot \cos\varphi} \cdot \left(1 - \frac{s_K}{l_f}\right) - F_{mu} \cdot \cos\varepsilon \cdot \left(1 - \frac{s_K + s_c}{l_f}\right) \tag{9}$$

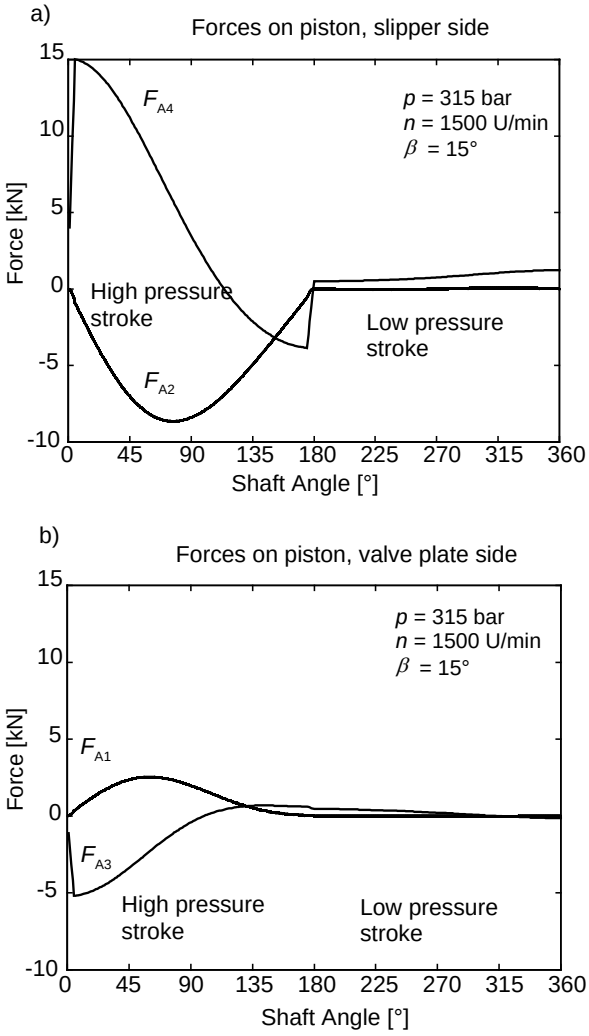

Fig. 3: *Calculated reaction forces*

These forces are acting in the corresponding co-ordinate directions e_1 to e_4. The co-ordinate system e_1 to e_4 shown in Fig. 3 is introduced to describe the eccentric motion of the piston in the gap with four degrees of freedom.

Figure 3 shows the forces F_{A1} to F_{A4} for one operating point of the machine. The pressure force F_{DK} causes a reaction force that acts always normal to the swash plate. Because the swash plate is fixed in the casing of the machine and the cylinder block rotates the reaction forces F_{A3} and F_{A4} are changing their algebraic sign during the high pressure stroke. The reaction forces F_{A1} and F_{A2} are reaching their maximum value at a shaft angle of approx. $\varphi = 90°$.

For the calculation of the forces the pressure in the displacement chamber is important. In an ideal pump with an ideal fluid the pressure p_K during the high pressure stroke is the same as in the high pressure port. During the low pressure stroke the pressure p_K is the

same as in the low pressure port. For several reasons the pressure in the displacement chamber is different from the ideal pressure. In a real pump operating with a viscous fluid throttle losses at the valve plate occur and there are compressibility and inertia effects affecting the pressure.

Therefore a difference of pressure in the ports of the machine and in the displacement chamber occurs.

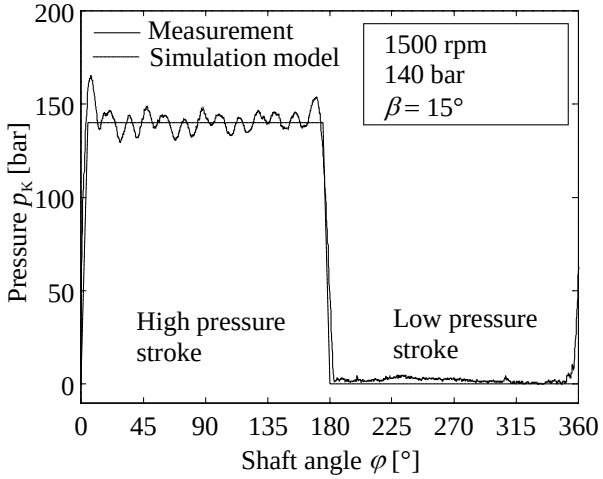

Fig. 4: *Instantaneous pressure in the displacement chamber*

Figure 4 shows the instantaneous pressure p_K that was measured in the displacement chamber. For the calculation of the temperatures the simplified pressure behaviour shown in Fig. 4 with a dash-dotted line is used. For the pressure gradient a linear behaviour over 5° shaft angle is assumed, which fits very good with the real pressure gradient measured in the machine.

3 Gap between Piston and Cylinder

The gap has two main functions. It works as a hydrodynamic bearing and as a sealing of the displacement chamber. Because of the eccentric motion of the piston in the cylinder, the resulting pressure distribution in the gap flow is also eccentric and can carry loads.

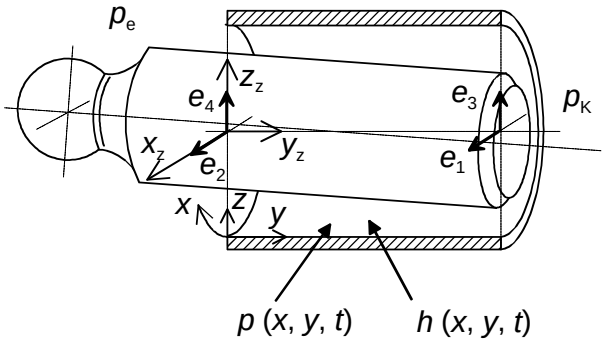

Fig. 5: *Gap between piston and cylinder*

Figure 5 shows the gap between piston and cylinder. The pressure distribution in the gap p and the gap height are depending on the place x, y and the time t. In the case of complete hydrodynamic lubrication, the forces resulting from the pressure distribution in the gap are equal to the forces acting on the piston. The pressure distribution can be computed in a plain x,y coordinate system with the Reynolds Equation (10) for an ideal smooth surface

$$\frac{\partial}{\partial x}\cdot\left(\frac{\partial p}{\partial x}\cdot\frac{h^3}{\mu}\right)+\frac{\partial}{\partial y}\cdot\left(\frac{\partial p}{\partial y}\cdot\frac{h^3}{\mu}\right)= 6\cdot\left(v_{Wx}\cdot\frac{\partial h}{\partial x}+v_{Wy}\cdot\frac{\partial h}{\partial y}+2\frac{\partial h}{\partial t}\right) \tag{10}$$

The calculation of the pressure distribution in the gap is done by solving the Reynolds Equation numerically with a finite volume method described in Patankar (1980). Therefore the Reynolds Equation is put into a discrete form and the resulting system of linear equations is solved by using the Gauss-Seidel method. The result is a discrete pressure distribution in the gap at each grid point *i,j*. When solving the Reynolds Equation mathematically, pressure equal or below zero can occur. However, this is not possible in a real flow. To avoid pressure values below zero, a simple method described in Krasser et al (1994) is used. While solving the linear system of equations with the Gauss-Seidel method, all pressure values below zero are set equal to zero. The lubricant viscosity μ depends very much on the local temperature in the gap. Therefore, the temperature is calculated later on to determine the local viscosity. For the calculation of the viscosity-temperature behaviour the equation described in Rodermund (1978):

$$\mu(\vartheta)=A\cdot\exp\left(\frac{B}{\vartheta+C}\right) \tag{11}$$

with

$$A=\mu_x\cdot\exp\left(-1.140089\cdot10^{-3}\cdot B\right) \tag{12}$$

and

$$B=159.56\cdot\ln\left(\frac{\mu_{40}}{\mu_x}\right) \tag{13}$$

is used. The viscosity μ_{40} is the viscosity of the oil at a temperature of ϑ = 40 °C and for $\mu_x = 1.8\cdot10^{-4}$ Pas is assumed. The value of *C* = 95 °C. For the calculation of the viscosity-pressure behaviour the equation as described in Ivantysyn and Ivantysynova (1993) is used:

$$\mu=\mu_0\cdot\exp\left(\alpha_P\cdot p\right) \tag{14}$$

were α_P is the viscosity-pressure coefficient and μ_0 is the viscosity at atmospheric pressure.

The local gap height can be well approximated by using the piston eccentricities.

$$h(x,y)=\frac{s_h}{2}-\left[e_2+(e_1-e_2)\frac{y}{l_f}\right]\cdot\sin\left(\frac{2x}{d_K}\right)+\left[e_4+(e_3-e_4)\frac{y}{l_f}\right]\cdot\cos\left(\frac{2x}{d_K}\right) \tag{15}$$

In the Reynolds Equation the squeeze film term $\partial h/\partial t$ occurs that can be calculated with the eccentric velocities of the piston.

$$\frac{\partial h}{\partial t}(x,y)=-\left[\dot e_2+(\dot e_1-\dot e_2)\frac{y}{l_f}\right]\cdot\sin\left(\frac{2x}{d_K}\right)+\left[\dot e_4+(\dot e_3-\dot e_4)\frac{y}{l_f}\right]\cdot\cos\left(\frac{2x}{d_K}\right) \tag{16}$$

If the resulting hydrodynamic forces are too small, the lubrication film is interrupted at some locations and solid to solid contact occurs. Because of the elastic properties of the parts, the piston and the cylinder are deformed under the influence of a contact pressure. For the calculation of the contact pressure it is necessary to solve the elastic contact equation. However this requires very extensive calculations. Several test runs have shown that the contact pressure is needed only for the reason of the stability of the numerical procedure. Under normal operating conditions of the pump no contact pressure occurs. Therefore, the contact pressure can be estimated. Once the gap height *h* is calculated at each grid point with Eq. (15), the elastic deformation is given as:

$$h_{el}(x,y)=\begin{cases}0 & \text{with } h\ge h_{min}\\ h_{min}-h & \text{with } h<h_{min}\end{cases} \tag{17}$$

For the reason of the stability for the computation of the pressure distribution, a minimal gap height of h_{min} = 0.2 µm is assumed. Table 1 shows the main parameters of the gap.

Table 1: Parameters of the gap

piston diameter	d_K	31.2 mm
inner piston diameter	d_{Ki}	13.2 mm
bushing length	l_f	68 mm
piston clearance	s_h	60 µm

The Young's modulus for the piston is E_K = $2.1\cdot10^{13}$ N/m². Making some assumptions about stress and the deformation of the piston the contact pressure p_{el} can be written as:

$$p_{el}=\frac{2\cdot E_K}{d_K-d_{Ki}}\cdot h_{el}=2.33\cdot10^{13}\cdot h_{el} \tag{18}$$

The total gap forces can be calculated as the sum of the hydrodynamic force and the contact pressure force. If both forces are computed at discrete grid points *i,j* the reaction forces of the gap can be summarised as follows:

$$F_{S1}=\sum_{i,j}-\Delta x_{i,j}\cdot\Delta y_{i,j}\cdot\left(p_{i,j}+p_{el\ i,j}\right)\cdot\left[\sin\left(\frac{2x_{i,j}}{d_K}\right)\cdot\frac{y_{i,j}}{l_f}\right] \tag{19}$$

$$F_{S2}=\sum_{i,j}-\Delta x_{i,j}\cdot\Delta y_{i,j}\cdot\left(p_{i,j}+p_{el\ i,j}\right)\cdot\left[\sin\left(\frac{2x_{i,j}}{d_K}\right)\cdot\left(1-\frac{y_{i,j}}{l_f}\right)\right] \tag{20}$$

$$F_{S3}=\sum_{i,j}\Delta x_{i,j}\cdot\Delta y_{i,j}\cdot\left(p_{i,j}+p_{el\ i,j}\right)\cdot\cos\left(\frac{2x_{i,j}}{d_K}\right)\cdot\frac{y_{i,j}}{l_f} \tag{21}$$

$$F_{S4}=\sum_{i,j}\Delta x_{i,j}\cdot\Delta y_{i,j}\cdot\left(p_{i,j}+p_{el\ i,j}\right)\cdot\cos\left(\frac{2x_{i,j}}{d_K}\right)\cdot\left(1-\frac{y_{i,j}}{l_f}\right) \tag{22}$$

The velocity v_y of the flow in the gap depending on the gap height z is given as:

$$v_y = \frac{1}{2\mu} \cdot \frac{\partial p}{\partial y} \cdot \left(z^2 - h \cdot z\right) + v_{\mathrm{Wy}} \cdot \frac{z}{h} \tag{23}$$

The leakage can be calculated by integrating the velocity field v_y in the gap over the piston circumference and the gap height:

$$Q_y = \int_0^{2\pi} \int_0^h v_y \, dz \, dx \tag{24}$$

Furthermore, Eq. (24) gives a good possibility to check the numerical procedure. It should compute the same value for Q_y at any section of the gap length y, because the condition of continuity has to be fulfilled over the piston length.

The friction forces can be calculated by integrating the shearing stress in the flow at the piston wall over the piston circumference and the gap length. The shearing stress in the flow can be calculated as:

$$\tau_y = \mu \cdot \frac{\partial v_y}{\partial z} \tag{25}$$

At the piston wall ($z = h$),

$$\tau_{\mathrm{Wy}} = \frac{h}{2} \cdot \frac{\partial p}{\partial y} + \mu \cdot \frac{v_{\mathrm{Wy}}}{h} \tag{26}$$

Integrating the shearing stress gives the axial friction force on the piston:

$$F_{\mathrm{Wy}} = \int_0^{2\pi} \int_0^l \tau_{\mathrm{Wy}} \, \mathrm{d}y \, \mathrm{d}\varphi_{\mathrm{K}} \tag{27}$$

3.1 Piston Motion

For the calculation of the eccentric motion of the piston under normal conditions it is necessary to solve the equations of motion which includes the accelerations. Here the inertial forces of the eccentric piston motion are very small compared to the forces $\boldsymbol{F}_{\mathrm{A}}$ and the forces $\boldsymbol{F}_{\mathrm{S}}$. Therefore, the inertial forces are neglected in this calculation. $\boldsymbol{F}_{\mathrm{A}}$ is the vector of the total forces acting on the piston. It depends on the time t. The forces of the gap $\boldsymbol{F}_{\mathrm{S}}$ are depending on the time. In addition, due to the hydrodynamic forces and the solid to solid contact forces, $\boldsymbol{F}_{\mathrm{S}}$ depends on the eccentric piston position $\boldsymbol{e}$ and the eccentric piston velocity $\dot{\boldsymbol{e}}$.

The procedure of the calculations is shown in Figure 6. At the operating point of the machine to be calculated, one revolution is separated in time steps $t^{(v)}$. At each time step the equilibrium of forces must be fulfilled. In the first time step, a eccentric position of the piston in the cylinder $\boldsymbol{e}^{(0)}$ is estimated. The eccentric velocity of the piston is varied until a velocity $\dot{\boldsymbol{e}}^{(0)}$ is found, so that the equilibrium of forces is fulfilled.

$$\mathbf{f}(\dot{\mathbf{e}}) = \mathbf{F}_{\mathrm{A}}\left(t\right) + \mathbf{F}_{\mathrm{S}}\left(t, \mathbf{e}, \dot{\mathbf{e}}\right) \overset{!}{=} 0 \tag{28}$$

To do so a value for the variable $\dot{\boldsymbol{e}}$ has to be found to make Eq. (28) equal to zero. Because Eq. (28) can be seen as a system of nonlinear equations with the independent variable $\dot{\boldsymbol{e}}$, a Newton method described in Engeln-Muellges (1990) for solving a nonlinear system of equations is used. After n steps $\dot{\boldsymbol{e}}^{(n)}$ has to be set as:

$$\dot{\boldsymbol{e}}^{(n)} = \dot{\boldsymbol{e}}^{(n-1)} + \Delta\dot{\boldsymbol{e}}^{(n)} \tag{29}$$

with

$$\Delta\dot{\boldsymbol{e}}^{(n)} = -\boldsymbol{J}^{-1}\left(\dot{\boldsymbol{e}}^{(n-1)}\right) \cdot \boldsymbol{f}\left(\dot{\boldsymbol{e}}^{(n-1)}\right) \tag{30}$$

The calculation of the vector $\boldsymbol{f}(\dot{\boldsymbol{e}})$ requires the solution of the Reynolds equation that has to be done numerically. Therefore, the matrix $\boldsymbol{J}$ cannot be computed directly and a difference method (Eq. 31) has to be used to obtain the values of $\boldsymbol{J}$.

$$\frac{\partial f_i}{\partial \dot{e}_j} = \frac{1}{\dot{e}_{\mathrm{h}}} \left\{ f_i\left(\dot{e}_1, .., \dot{e}_j, .., \dot{e}_4\right) - f_i\left(\dot{e}_1, .., \dot{e}_j - \dot{e}_{\mathrm{h}}, .., \dot{e}_4\right) \right\} \tag{31}$$

with i=1, 2, 3, 4 and j=1, 2, 3, 4.

In this method the value of $\dot{e}_{\mathrm{h}}$ is not easy to obtain. Test runs have shown that values of $\dot{e}_{\mathrm{h}} = 10^{-5}$ to 10^{7} m/s are a good choice, depending on the operation parameters of the machine. The Newton method is stopped, when the condition

$$\left\| \boldsymbol{f}\left(\dot{\boldsymbol{e}}^{(n)}\right) \right\| \le F_{\mathrm{Abbr.}} = 0.01 \text{ N} \tag{32}$$

is fulfilled. $F_{\mathrm{Abbr.}}$ is the error that is left in the equilibrium of forces.

Once the Newton method has stopped successfully, the eccentric position of the piston can be calculated for the new time step $t^{(v+1)}$ by numerically integrating the velocity over the time step.

$$\boldsymbol{e}^{(v+1)} = \boldsymbol{e}^{(v)} + \dot{\boldsymbol{e}}^{(v)} \cdot \left(t^{(v+1)} - t^{(v)}\right) \tag{33}$$

Equation (33) is the so called Euler-method for solving ordinary differential equations. The corresponding computer program uses more efficient methods that are included in a numerical library for solving the ordinary differential equations. Test runs have shown that methods for solving stiff differential equations are useful.

Starting the Newton method again, a new eccentric piston velocity $\dot{\boldsymbol{e}}^{(v+1)}$ can be found in the next time step. Making the time step small enough, one can ensure that the eccentric velocity of the piston calculated in the previous time step $t^{(v)}$ is a good approximation for the eccentric velocity to be calculated in the present time step $t^{(v+1)}$. Because of the local convergence of the Newton method, the step size has to be chosen small enough to ensure convergence. Practical test have shown that a step size corresponding to a shaft angle of $\Delta\varphi$ = 2 to 5° is sufficiently small enough for normal operating conditions of the machine. To shorten computing time the step size can be extended up to a corresponding shaft angle of $\Delta\varphi$ = 10 to 20° in low pressure stroke.

3.2 Numerical Procedure for Calculating the Piston Motion

One can establish an iterative method for the calculation of the motion of the piston within the gap. Figure 6 shows the diagram for the calculations. The calculation starts at $\varphi = 0°$. At the beginning ($v = 0$) the position $\boldsymbol{e}^{(v)}$ and the velocity $\dot{\boldsymbol{e}}^{(v)}$ of the piston is not known and have to be guessed. After doing that the forces $\boldsymbol{F}_A$ and $\boldsymbol{F}_S$ can be calculated using the equations (6) to (9) and (19) to (22). The velocity $\dot{\boldsymbol{e}}^{(v)}$ is then corrected with the Newton method until the equilibrium of force in Eq. (28) is fulfilled. Then the time step is increased and the position of the piston at the new time step $\boldsymbol{e}^{(v+1)}$ is calculated by numerically integrating the piston velocity $\dot{\boldsymbol{e}}^{(v)}$. Then a new velocity $\dot{\boldsymbol{e}}^{(v+1)}$ is calculated with the Newton method that fits the equilibrium of forces for this time step.

The criterion for stopping the calculations is the piston position $\boldsymbol{e}$ at a shaft angle of $\varphi = 0°$ and $\varphi = 360°$. Because the piston undergoes a continuous motion in the gap the calculated positions at $\varphi = 0°$ and $\varphi = 360°$ should be the same. The calculation is therefore done for several revolutions for the cylinder block until this is reached.

Another reason for calculating several revolutions of the cylinder block is that the steady state temperature distribution in the assembly is calculated after each completed revolution. The calculation of the piston motion is therefore continued until the temperature distribution in the assembly does not differ from one revolution to another.

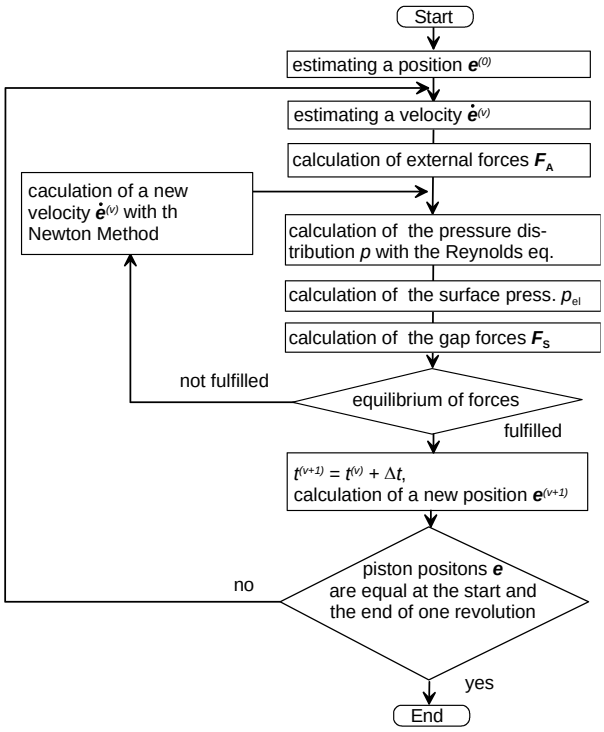

Fig. 6: *Procedure for the calculations*

4 Temperature Distribution

In the gap flow energy is dissipated to heat. This leads to a heating of the flow and the solid parts of the assembly. After a time a equilibrium is reached between the dissipated energy and the heat carried off by convection due to the flow and diffusion through the solid parts and a static temperature distribution in the assembly is reached.

Figure 7 shows the assembly and the three-dimensional grid that is used to calculate the temperatures. The three-dimensional heat transfer in the assembly is described by the energy equation with the convection term on the right hand side and the diffusion term and the source term on the left hand side (Ivantysynova 1985).

$$\rho \cdot c_p \cdot \left(\frac{\partial T}{\partial t} + v_x \cdot \frac{\partial T}{\partial x} + v_y \cdot \frac{\partial T}{\partial y} \right) = \lambda \cdot \left(\frac{\partial^2 T}{\partial x^2} + \frac{\partial^2 T}{\partial y^2} + \frac{\partial^2 T}{\partial z^2} \right) + \phi_D \tag{34}$$

Once the laminar gap flow is computed, the energy losses in the flow can be calculated with the dissipation function ϕ_D. The density ρ, the specific heat capacity c_p and the thermal conductivity λ are not constant over the assembly but differ with the materials. Table 2 shows the properties of the materials that are used in the assembly.

Solving the energy equation with a numerical method described in Patankar (1980) gives the temperature distribution in the assembly and especially in the gap. The flow in the gap changes much faster than the temperatures in the assembly. Therefore, the data of the gap flow is averaged over one revolution of the shaft and the calculation of the temperature distribution is done after the calculation of the gap flow.

On the boundaries of the thermal model the appropriate boundary conditions have to be defined. At the areas that are in contact with oil, heat is transferred from the cylinder block to the oil. The heat transfer can be calculated with the heat transfer coefficient α. It considers the properties of the oil and the turbulent flow in the casing of the machine. Because there is no boundary layer in the flow in the casing the value of α has to be gained by comparison between measurement and simulation. For this machine a value of $\alpha = 1000$ W/(m²K) is sufficient. Since the thermal conditions are the same around every piston in the cylinder block a radial cut in the block is allowed. The model calculates the correct temperature at each grid element when the appropriate neighbour on the opposite side of the model is considered.

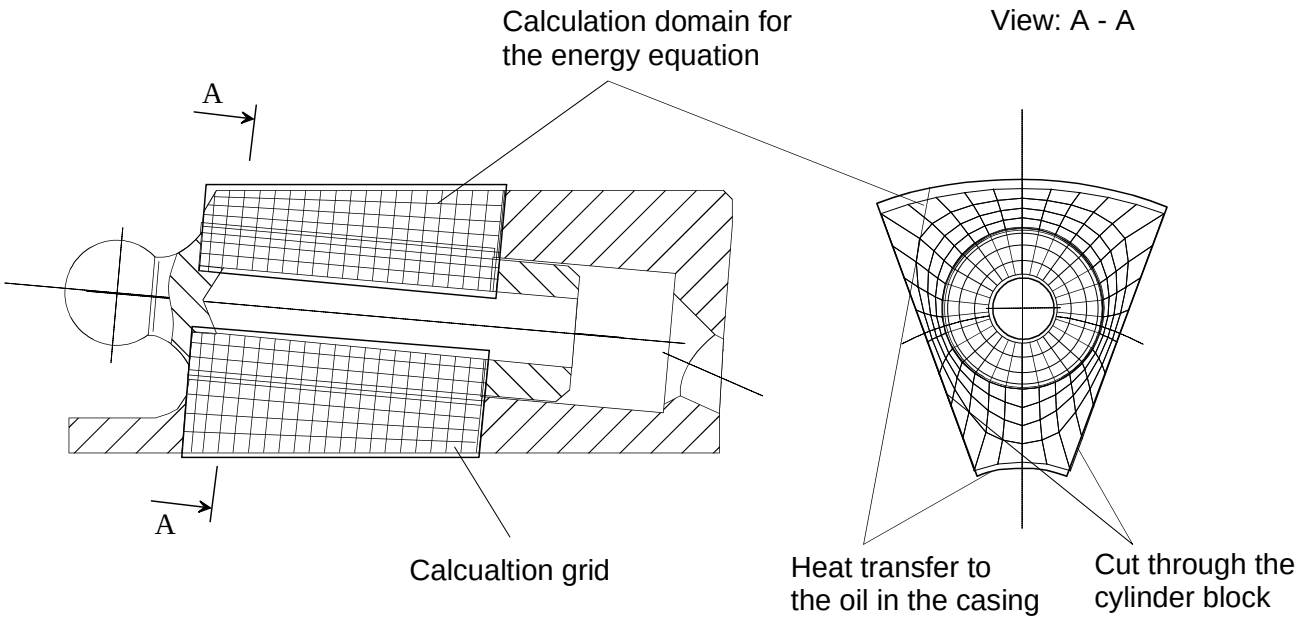

Fig. 7: *Calculation domain for the thermal model*

Table 2: Properties of the materials

	density ρ[kg/m³]	spec. heat capacity c_P [J/(kg K)]	thermal conductivity λ[W/mK]
piston	7850	490	50.28
cylinder	7850	490	41.9
bushing	8100	390	63
oil HLP32	862.1	1880	0.1

5 Experimental Investigations

The simulation model is based on experimental investigations that were made on a standard axial piston pump. The pump has been modified to measure the temperature distribution in the cylinder block and the dynamic pressure inside the displacement chamber under normal operating conditions. Figure 8 shows the pump used for the measurements. The top ends of the thermocouples are placed at the gap to measure the temperature directly at the gap surface. The piezoelectric pressure sensor is placed at the displacement chamber. The thermocouples and the pressure sensor are connected via a connection disk with the rotor of the

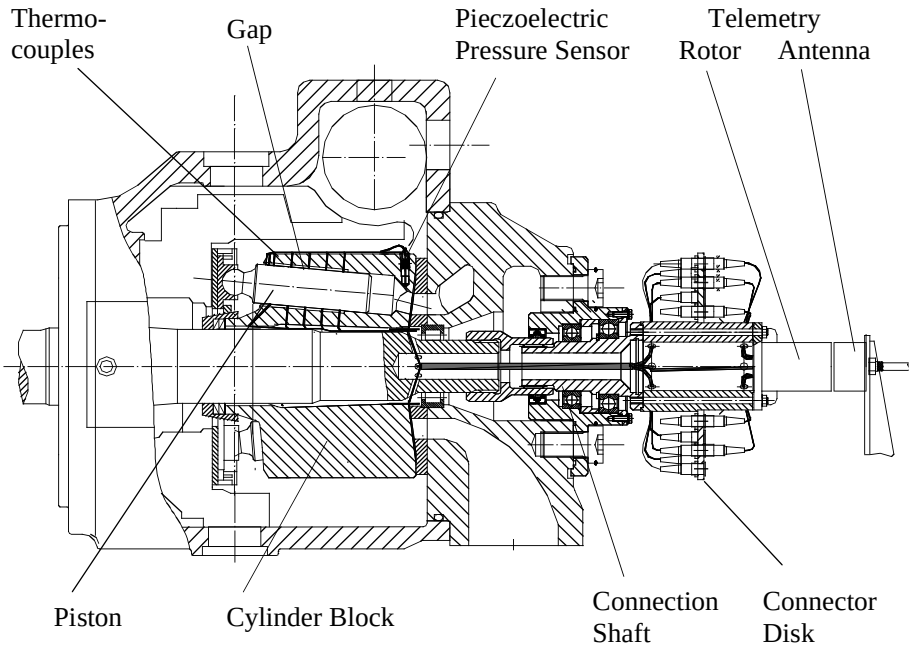

Fig. 8: *Axial piston pump modified for measurement of the temperature distribution in the cylinder block and the dynamic pressure in the displacement chamber.*

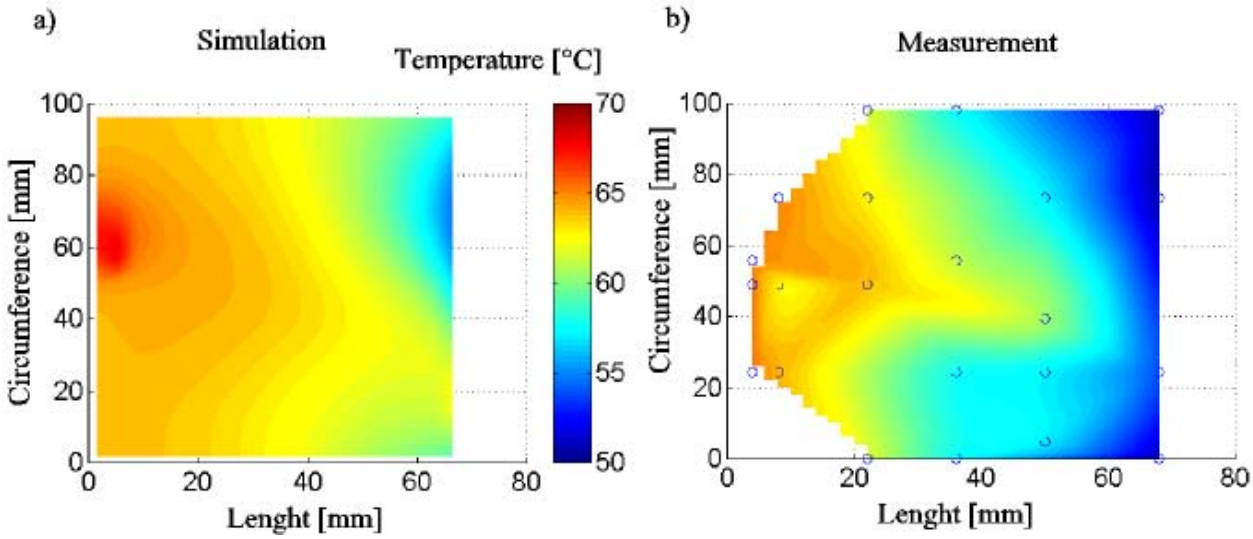

Fig. 9: *Temperature distribution in the gap (Simulation and Measurement, 1500 rpm, β = 15°, 140 bar, suction oil T_{suc} = 50°C, leakage oil T_{leak} = 61°C)*

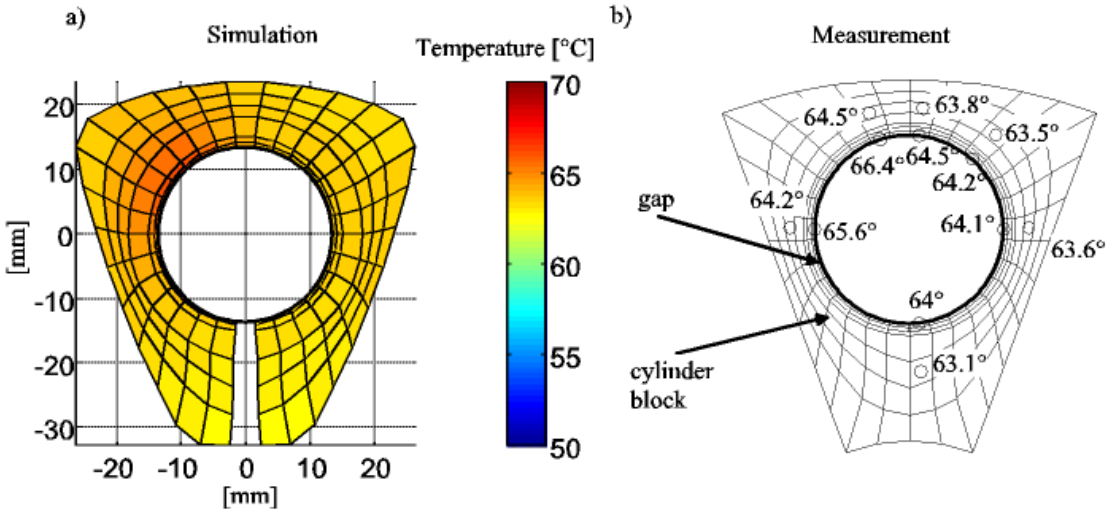

Fig. 10: *Temperature distribution in the assembly near the slipper side*

telemetry. It works as a measuring amplifier and gives back the temperatures and the dynamic pressure in the displacement chamber. The connection disk is necessary because 60 thermocouples are placed in the cylinder block and the telemetry has got only 19 channels. The measurement data are send to the antenna and then transferred to a computer that analyses the data and saves it to disk. Table 3 shows the specifications of the measurement equipment that was used for the measurements.

Table 3: Measurement equipment

Sensor	Amplifier	Analog to Digital-converter
thermocouples, Philips Thermo-coax, Ni/CrNi, Type K, class 1 (±1.5°C)*	Manner, 19 channels serial, integrated in telemetry, Linearity: < 0.1% accuracy: 0.01% / °C	Keithley, DAS 1802ST-DA, 333 KHz / 12 Bit, 16 channels
piezoelectric pressure sensor, Kistler 6005, eigenfrequency: 140 kHz	Kistler 5042Q1, 1 channel, integrated in telemetry, range 0.1 Hz to 10 kHz	

* The accuracy of the thermocouples is assumed to be better than ± 1.5 °C. Comparative measurements have shown differences in the temperatures at about ± 0.2 °C.

The measurements were made for different operating parameters of the machine such as swash plate angle ß, speed and pressure. The measurement data was recorded after a steady state in the leakage temperature and in the temperatures of the cylinder block was reached.

6 Results

With the described model it is possible to calculate the gap flow, the eccentric piston motion in the gap and the temperatures in the complete piston cylinder assembly. The calculations are based on the design and the operating parameters of the machine. The model is verified with measurements that were made in the assembly of a standard machine.

Figure 9 shows a temperature field that has been calculated and measured for one operating point of the machine. At the slipper side the gap is in contact with oil in the displacement chamber. Because the direction of the leakage flow is from the valve plate side to the slipper side of the gap, the temperature increases in this

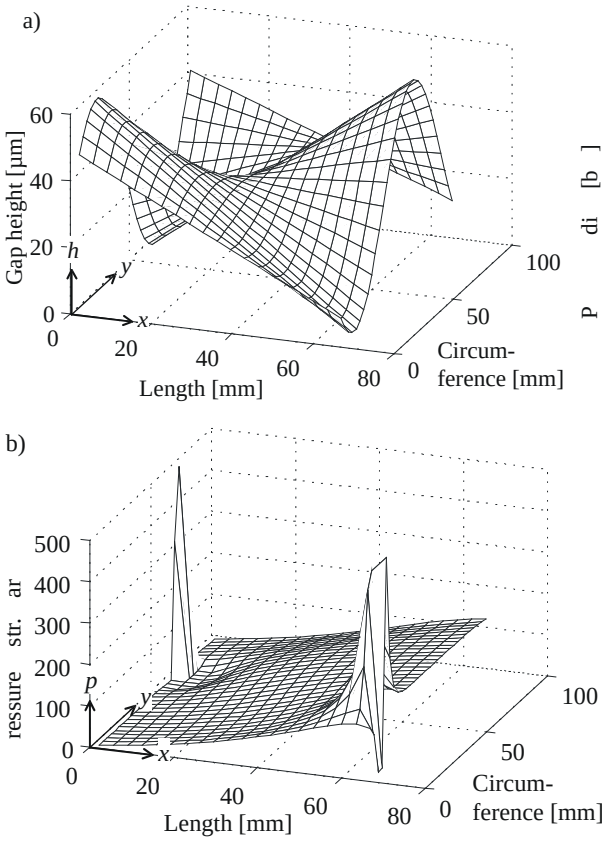

Fig. 11: *Gap geometry and pressure distribution*

direction. Both simulation Fig. 10 (a) and measurement Figure 10 (b) show the increase of the temperatures. It can be seen also that the temperatures are not equal along the gap circumference. This is because of the

eccentric position of the piston in the cylinder bushing. At locations in the gap with a very small gap height in Fig. 11 (a) energy dissipation is high and the convective heat transfer is low. This leads to increasing temperatures. At locations with a wide gap height energy dissipation is low and the convective heat transport is high due to the high flow.

Figure 10 shows the temperature distribution in the assembly in a cutaway view near the slipper side. Figure 10 (a) shows the calculated temperatures and Fig. 10 (b) the measured ones. It can be seen that the temperature of the oil in the gap is higher than the temperatures of the cylinder block and the piston. Therefore, heat is transferred from the gap flow to the cylinder block and the piston in this area. Because of the eccentric movement of the piston in the cylinder block is not symmetric the temperatures differ with the gap circumference. It can be seen that a good conformance between measurement and simulation is achieved with the described simulation model.

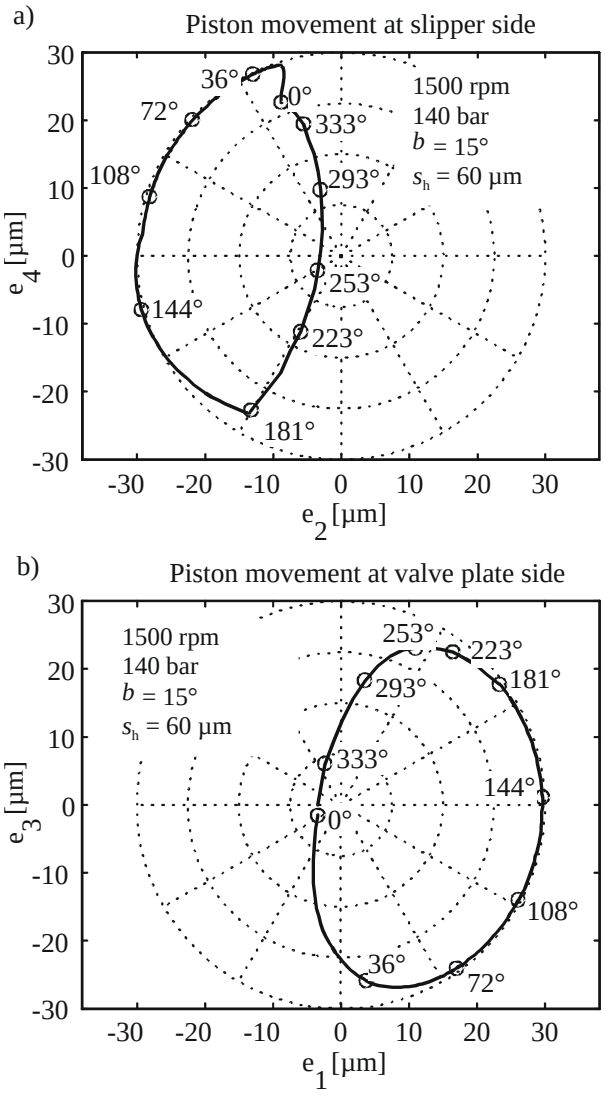

Fig. 12: *Piston motion*

In Figure 11 the gap height and the pressure distribution calculated for this gap height for one step (φ = 90°) is shown. On both locations with very small gap height, the pressure computed with the model increases up to 500 bar. Despite of the severe loads in this operating point, the computed gap height does not fall below the minimal gap height h_{min} = 0.2 µm and mechanical contact does not occur at all time.

The computed very high pressure peaks seem to be very unlikely due to the elastic properties of the parts. For further models it seems to be necessary to include the so called elastohydrodynamic calculation in the model. It considers the elastic properties of the parts in the assembly. However, this brings a very extensive numerical calculation and cannot be done today without some simplifications.

The motion of the piston in the cylinder can be shown in diagrams that plot the position of the piston axis in the cylinder bore. Because of the four degrees of freedom the motion of the piston is described clearly in two diagrams. Figure 12 shows the motion of the piston for rotating angles from φ = 0° to 360°. The minimal gap heights occur at angles from φ = 0° to 180°, because of the severe loads acting on the piston during high pressure operation.

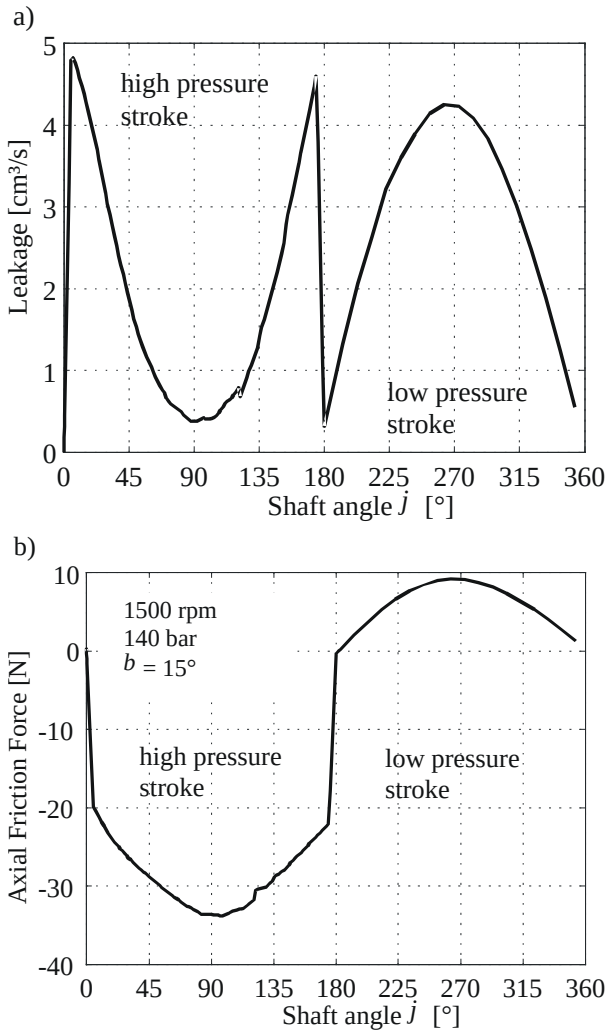

Fig. 13: *Axial friction forces and piston leakage*

Figure 13 (a) shows the calculated leakage of the piston cylinder assembly over one revolution of the shaft. In pumping mode the piston moves against the pressure gradient between the displacement chamber and the casing of the machine and the leakage reaches a

minimum at the highest piston velocity at a shaft angle of $\varphi = 90°$ in the high pressure stroke. At the outer and the inner dead center the leakage reaches its maximum because the piston velocity is very low. At low pressure stroke there is almost no pressure difference and the leakage follows almost the piston velocity.

The influence of the piston motion and the pressure difference on the axial friction forces can be seen in Fig. 13 (b). During the high pressure stroke the leakage occurs that is driven by the pressure difference between displacement chamber and the casing of the machine. This leads to a high shearing stress on the piston wall and a high friction force. During the low pressure stroke there is almost no pressure difference. Therefore, the shearing stress caused by the pressure flow is very small. The influence of the pressure flow can be seen at the dead center points near $\varphi = 0°$ and $\varphi = 180°$ were there is almost no axial motion of the piston. The other important influence on the axial friction force is the shearing stress caused by the motion of the piston in axial direction. It is high at shaft angles of $\varphi = 90°$ and $\varphi = 270°$ and it is zero at the dead center points. Note that the friction forces caused by the pressure flow and the motion of the piston are acting in the same direction during high pressure stroke in pumping mode.

7 Conclusion

A precise method for calculating the nonisothermal gap flow between piston and cylinder in swash plate type axial piston machines has been developed. This method requires the simultaneous calculation of the equations of motion for the piston and the non-isothermal gap flow described by the Reynolds equation and the energy equation. The Reynolds equation and the energy equation are partial differential equations that are computed numerically by establishing a finite volume method. Solving the Reynolds equation requires the knowledge of the eccentric position and velocity of the piston. It is used to calculate the hydrodynamic forces that are acting on the piston. But for the calculation of the equations of motion it is necessary to know all the forces that are acting on the piston. The proposed model contains an iterative method to calculate both parts simultaneously.

The temperature distribution in the gap has an influence on the viscosity of the oil and on the gap flow. With the proposed thermal model it is possible to calculate the temperature distribution in the whole assembly based on the case temperature of the machine. Additional measurements that have been made by the author have shown that there is a good conformance between the measured and the calculated temperature distribution in the gap even at different operating parameters of the machine.

Nomenclature

a_c	Coriolis acceleration	[m/s²]
a_K	piston acceleration in *y*-direction	[m/s²]
a_u	centrifugal piston acceleration	[m/s²]
c_p	specific heat capacity	[J/(kgK)]
d_K	piston diameter	[m]
d_{Ki}	inner piston diameter	[m]
E_K	Young's modulus of the piston	[N /m²]
$e_{1..4}$	eccentric piston position	[m]
$\dot{e}_{1..4}$	eccentric piston velocity	[m/s]
$\dot{e}_h$	variation in eccentric piston velocity	[m/s]
$F_{A1..4}$	sum of the external forces	[N]
F_{Abbr}	error in equilibrium of forces	[N]
.		
F_{DK}	pressure force	[N]
F_{mc}	Coriolis force	[N]
F_{mK}	inertia force in *y*-direction	[N]
F_{mu}	centrifugal force	[N]
F_{RK}	sum of axial piston forces	[N]
$F_{S1..4}$	gap forces	[N]
F_{SK}	reaction force of the swash plate	[N]
F_{WKy}	piston friction force	[N]
h	local gap height	[m]
h_{el}	bulk elastic deformation	[m]
h_{min}	minimal gap height	[m]
l_f	bushing length	[m]
$\boldsymbol{J}$	matrix of partial derivatives	
m_K	mass of piston and slipper	[kg]
n	index for Newton method	[-]
p	local pressure	[Pa]
p_e	pressure in casing of the machine	[Pa]
p_{el}	surface pressure due to elastic deformation	[Pa]
p_K	pressure in displacement chamber	[Pa]
s_c	distance between piston ball and center of mass	[m]
s_h	piston clearance	[m]
T	temperature	[°C]
t	time	[s]
v	index for the numerical integration	[-]
v_W	relative velocity between piston and cylinder	[m/s]
$x..z$	system of coordinates for the gap	[m]
$x_Z..z_Z$	system of coordinates for the cylinder block	[m]
β	swash plate angle	[°]
ε	pitch between piston axis and shaft	[°]
ϕ_D	local energy losses in the gap	[W/m³]
φ	shaft angle	[°]
μ	viscosity	[Pas]
λ	thermal conductivity	[W/(mK)]
ρ	density	[kg/m³]
τ	shearing stress	[N/m²]
ω	shaft speed	[rad/s]

References

Berge, M. 1983. *Computational Model of Non-isothermal Gap Flow* (Slovak). PhD Thesis, TU Bratislava, Slovakia.

Engeln-Muellges, G. 1990. *Formelsammlung zur numerischen Mathematik mit C-Programmen*. Mannheim: Wissenschaftsverlag.

Ivantysyn, J. and **Ivantysysnova, M.** 1993. *Hydrostatische Pumpen und Motoren*. 1. Aufl., Würzburg: Vogel Verlag.

Ivantysynova, M. 1985. Temperaturfeld im Schmierspalt zwischen Kolben und Zylinder einer Axialkolbenmaschine. *Maschinenbautechnik*. 34, pp. 532-535.

Ivantysynova, M. 1999a. Ways for Efficiency Improvements of Modern Displacement Machines. *6th Scandinavian Intern. Conf. on Fluid Power*. Tampere, Finnland.

Ivantysynova, M. 1999b. A New Approach to the Design of Sealing and Bearing Gaps of Displacement Machines. *4th JHPS International Symposium on Fluid Power*. Tokyo, Japan.

Kleist, A. 1995. Berechnung von hydrostatischen Dichtstellen in hydraulischen Maschinen. *Ölhydraulik und Pneumatik.* 39, pp 767-771.

Krasser, J., Laback, O., Loibennegger B. und **Priebsch, H.** 1994. Anwendung eines elastohydrodynamischen Verfahrens zur Berechnung von Kurbeltriebslagern. *Motortechnische Zeitschrift* 55, pp. 656-663.

Olems, L. and **Ivantysynova, M.** 1998. Investigation of the cylinder / piston temperature behaviour in axial piston pumps. *Proceedings of 1st Bratislavian Fluid Power Symposium*, Bratislava, Slovakia.

Olems, L. 1999. Entwicklung eines nichtisothermen Simulationsmodells zur Berechnung des Spaltes der Kolben- Zylinderbaugruppe bei Axialkolbenmaschinen. *Ölhydraulik und Pneumatik*. 43 No.11/12, pp. 833-839.

Patankar, S. V. 1980. *Numerical Heat Transfer and Fluid Flow*. New York, Washington: Hemisphere Publishing Corporation.

Renius, K. T. 1974. *Untersuchung zur Reibung zwischen Kolben und Zylinder bei Schrägscheiben- Axialkolbenmaschinen.* VDI-Forschungsheft 561.

Rodermund, H. 1978. Berechnung der Temperaturabhängigkeit der Viskosität von Mineralölen aus dem Viskositätsgrad. *Schmiertechnik und Tribologie*. 25, pp. 56-57.

Vogelpohl, G. 1937. *Beiträge zur Kenntnis der Gleitlagerreibung*. VDI-Forschungsheft Nr. 386. Berlin: VDI-Verlag.

Lars Olems
Born on February 23th 1969 in Schorndorf (Germany) Study of Mechanical Engineering at the TU Hamburg-Harburg. Diploma Thesis at the Bayer AG. Scientific Employee at the Department of Measurement and Control Engineering of the Gerhard Mercator University of Duisburg. Scientific Employee at the Institute for Aircraft Systems Engineering at the Technical University of Hamburg-Harburg.